

MIT Open Access Articles

*Measurement of the semileptonic branching
fraction of the B_s meson*

The MIT Faculty has made this article openly available. **Please share**
how this access benefits you. Your story matters.

Citation: "Measurement of the semileptonic branching fraction of the B_s meson."
Physical Review D, 85 (2012): [9 pages]. © 2012 American Physical Society.

As Published: <http://dx.doi.org/10.1103/PhysRevD.85.011101>

Publisher: American Physical Society

Persistent URL: <http://hdl.handle.net/1721.1/70552>

Version: Final published version: final published article, as it appeared in a journal, conference proceedings, or other formally published context

Terms of Use: Article is made available in accordance with the publisher's policy and may be subject to US copyright law. Please refer to the publisher's site for terms of use.



Measurement of the semileptonic branching fraction of the B_s meson

J. P. Lees,¹ V. Poireau,¹ V. Tisserand,¹ J. Garra Tico,² E. Grauges,² M. Martinelli,^{3a,3b} D. A. Milanes,^{3a} A. Palano,^{3a,3b} M. Pappagallo,^{3a,3b} G. Eigen,⁴ B. Stugu,⁴ D. N. Brown,⁵ L. T. Kerth,⁵ Yu. G. Kolomensky,⁵ G. Lynch,⁵ H. Koch,⁶ T. Schroeder,⁶ D. J. Asgeirsson,⁷ C. Hearty,⁷ T. S. Mattison,⁷ J. A. McKenna,⁷ A. Khan,⁸ V. E. Blinov,⁹ A. R. Buzykaev,⁹ V. P. Druzhinin,⁹ V. B. Golubev,⁹ E. A. Kravchenko,⁹ A. P. Onuchin,⁹ S. I. Serednyakov,⁹ Yu. I. Skovpen,⁹ E. P. Solodov,⁹ K. Yu. Todyshev,⁹ A. N. Yushkov,⁹ M. Bondioli,¹⁰ D. Kirkby,¹⁰ A. J. Lankford,¹⁰ M. Mandelkern,¹⁰ D. P. Stoker,¹⁰ H. Atmacan,¹¹ J. W. Gary,¹¹ F. Liu,¹¹ O. Long,¹¹ G. M. Vitug,¹¹ C. Campagnari,¹² T. M. Hong,¹² D. Kovalskyi,¹² J. D. Richman,¹² C. A. West,¹² A. M. Eisner,¹³ J. Kroseberg,¹³ W. S. Lockman,¹³ A. J. Martinez,¹³ T. Schalk,¹³ B. A. Schumm,¹³ A. Seiden,¹³ C. H. Cheng,¹⁴ D. A. Doll,¹⁴ B. Echenard,¹⁴ K. T. Flood,¹⁴ D. G. Hitlin,¹⁴ P. Ongmongkolkul,¹⁴ F. C. Porter,¹⁴ A. Y. Rakitin,¹⁴ R. Andreassen,¹⁵ M. S. Dubrovin,¹⁵ Z. Huard,¹⁵ B. T. Meadows,¹⁵ M. D. Sokoloff,¹⁵ L. Sun,¹⁵ P. C. Bloom,¹⁶ W. T. Ford,¹⁶ A. Gaz,¹⁶ M. Nagel,¹⁶ U. Nauenberg,¹⁶ J. G. Smith,¹⁶ S. R. Wagner,¹⁶ R. Ayad,^{17,*} W. H. Toki,¹⁷ B. Spaan,¹⁸ M. J. Kobel,¹⁹ K. R. Schubert,¹⁹ R. Schwierz,¹⁹ D. Bernard,²⁰ M. Verderi,²⁰ P. J. Clark,²¹ S. Playfer,²¹ D. Bettoni,^{22a} C. Bozzi,^{22a} R. Calabrese,^{22a,22b} G. Cibinetto,^{22a,22b} E. Fioravanti,^{22a,22b} I. Garzia,^{22a,22b} E. Luppi,^{22a,22b} M. Menerato,^{22a,22b} M. Negrini,^{22a,22b} L. Piemontese,^{22a} V. Santoro,^{22a,22b} R. Baldini-Ferrolì,²³ A. Calcaterra,²³ R. de Sangro,²³ G. Finocchiaro,²³ M. Nicolaci,²³ P. Patteri,²³ I. M. Peruzzi,^{23,†} M. Piccolo,²³ M. Rama,²³ A. Zallo,²³ R. Contri,^{24a,24b} E. Guido,^{24a,24b} M. Lo Vetere,^{24a,24b} M. R. Monge,^{24a,24b} S. Passaggio,^{24a} C. Patrignani,^{24a,24b} E. Robutti,^{24a} B. Bhuyan,²⁵ V. Prasad,²⁵ C. L. Lee,²⁶ M. Morii,²⁶ A. J. Edwards,²⁷ A. Adametz,²⁸ J. Marks,²⁸ U. Uwer,²⁸ F. U. Bernlochner,²⁹ H. M. Lacker,²⁹ T. Lueck,²⁹ P. D. Dauncey,³⁰ M. Tibbetts,³⁰ P. K. Behera,³¹ U. Mallik,³¹ C. Chen,³² J. Cochran,³² W. T. Meyer,³² S. Prell,³² E. I. Rosenberg,³² A. E. Rubin,³² A. V. Gritsan,³³ Z. J. Guo,³³ N. Arnaud,³⁴ M. Davier,³⁴ D. Derkach,³⁴ G. Grosdidier,³⁴ F. Le Diberder,³⁴ A. M. Lutz,³⁴ B. Malaescu,³⁴ P. Roudeau,³⁴ M. H. Schune,³⁴ A. Stocchi,³⁴ G. Wormser,³⁴ D. J. Lange,³⁵ D. M. Wright,³⁵ I. Bingham,³⁶ C. A. Chavez,³⁶ J. P. Coleman,³⁶ J. R. Fry,³⁶ E. Gabathuler,³⁶ D. E. Hutchcroft,³⁶ D. J. Payne,³⁶ C. Touramanis,³⁶ A. J. Bevan,³⁷ F. Di Lodovico,³⁷ R. Sacco,³⁷ M. Sigamani,³⁷ G. Cowan,³⁸ D. N. Brown,³⁹ C. L. Davis,³⁹ A. G. Denig,⁴⁰ M. Fritsch,⁴⁰ W. Gradl,⁴⁰ A. Hafner,⁴⁰ E. Prencipe,⁴⁰ K. E. Alwyn,⁴¹ D. Bailey,⁴¹ R. J. Barlow,^{41,‡} G. Jackson,⁴¹ G. D. Lafferty,⁴¹ E. Behn,⁴² R. Cenci,⁴² B. Hamilton,⁴² A. Jawahery,⁴² D. A. Roberts,⁴² G. Simi,⁴² C. Dallapiccola,⁴³ R. Cowan,⁴⁴ D. Dujmic,⁴⁴ G. Sciolla,⁴⁴ D. Lindemann,⁴⁵ P. M. Patel,⁴⁵ S. H. Robertson,⁴⁵ M. Schram,⁴⁵ P. Biassoni,^{46a,46b} N. Neri,^{46a,46b} F. Palombo,^{46a,46b} S. Stracka,^{46a,46b} L. Cremaldi,⁴⁷ R. Godang,^{47,§} R. Kroeger,⁴⁷ P. Sonnek,⁴⁷ D. J. Summers,⁴⁷ X. Nguyen,⁴⁸ M. Simard,⁴⁸ P. Taras,⁴⁸ G. De Nardo,^{49a,49b} D. Monorchio,^{49a,49b} G. Onorato,^{49a,49b} C. Sciacca,^{49a,49b} G. Raven,⁵⁰ H. L. Snoek,⁵⁰ C. P. Jessop,⁵¹ K. J. Knoepfel,⁵¹ J. M. LoSecco,⁵¹ W. F. Wang,⁵¹ K. Honscheid,⁵² R. Kass,⁵² J. Brau,⁵³ R. Frey,⁵³ N. B. Sinev,⁵³ D. Strom,⁵³ E. Torrence,⁵³ E. Feltresi,^{54a,54a} N. Gagliardi,^{54a,54b} M. Margoni,^{54a,54b} M. Morandin,^{54a} M. Posocco,^{54a} M. Rotondo,^{54a} F. Simonetto,^{54a,54b} R. Stroili,^{54a,54b} S. Akar,⁵⁵ E. Ben-Haim,⁵⁵ M. Bomben,⁵⁵ G. R. Bonneaud,⁵⁵ H. Briand,⁵⁵ G. Calderini,⁵⁵ J. Chauveau,⁵⁵ O. Hamon,⁵⁵ Ph. Leruste,⁵⁵ G. Marchiori,⁵⁵ J. Ocariz,⁵⁵ S. Sitt,⁵⁵ M. Biasini,^{56a,56b} E. Manoni,^{56a,56b} S. Pacetti,^{56a,56b} A. Rossi,^{56a,56b} C. Angelini,^{57a,57b} G. Batignani,^{57a,57b} S. Bettarini,^{57a,57b} M. Carpinelli,^{57a,57b,||} G. Casarosa,^{57a,57b} A. Cervelli,^{57a,57b} F. Forti,^{57a,57b} M. A. Giorgi,^{57a,57b} A. Lusiani,^{57a,57c} B. Oberhof,^{57a,57b} E. Paoloni,^{57a,57b} A. Perez,^{57a} G. Rizzo,^{57a,57b} J. J. Walsh,^{57a} D. Lopes Pegna,⁵⁸ C. Lu,⁵⁸ J. Olsen,⁵⁸ A. J. S. Smith,⁵⁸ A. V. Telnov,⁵⁸ F. Anulli,^{59a} G. Cavoto,^{59a} R. Faccini,^{59a,59b} F. Ferrarotto,^{59a} F. Ferroni,^{59a,59b} M. Gaspero,^{59a,59b} L. Li Gioi,^{59a} M. A. Mazzoni,^{59a} G. Piredda,^{59a} F. Renga,^{59a,59b} C. Büniger,⁶⁰ O. Grünberg,⁶⁰ T. Hartmann,⁶⁰ T. Leddig,⁶⁰ H. Schröder,⁶⁰ R. Waldi,⁶⁰ T. Adye,⁶¹ E. O. Olaiya,⁶¹ F. F. Wilson,⁶¹ S. Emery,⁶² G. Hamel de Monchenault,⁶² G. Vasseur,⁶² Ch. Yèche,⁶² D. Aston,⁶³ D. J. Bard,⁶³ R. Bartoldus,⁶³ C. Cartaro,⁶³ M. R. Convery,⁶³ J. Dorfan,⁶³ G. P. Dubois-Felsmann,⁶³ W. Dunwoodie,⁶³ M. Ebert,⁶³ R. C. Field,⁶³ M. Franco Sevilla,⁶³ B. G. Fulsom,⁶³ A. M. Gabareen,⁶³ M. T. Graham,⁶³ P. Grenier,⁶³ C. Hast,⁶³ W. R. Innes,⁶³ M. H. Kelsey,⁶³ H. Kim,⁶³ P. Kim,⁶³ M. L. Kocian,⁶³ D. W. G. S. Leith,⁶³ P. Lewis,⁶³ B. Lindquist,⁶³ S. Luitz,⁶³ V. Luth,⁶³ H. L. Lynch,⁶³ D. B. MacFarlane,⁶³ D. R. Muller,⁶³ H. Neal,⁶³ S. Nelson,⁶³ M. Perl,⁶³ T. Pulliam,⁶³ B. N. Ratcliff,⁶³ A. Roodman,⁶³ A. A. Salnikov,⁶³ R. H. Schindler,⁶³ A. Snyder,⁶³ D. Su,⁶³ M. K. Sullivan,⁶³ J. Va'vra,⁶³ A. P. Wagner,⁶³ M. Weaver,⁶³ W. J. Wisniewski,⁶³ M. Wittgen,⁶³ D. H. Wright,⁶³ H. W. Wulsin,⁶³ A. K. Yarritu,⁶³ C. C. Young,⁶³ V. Ziegler,⁶³ W. Park,⁶⁴ M. V. Purohit,⁶⁴ R. M. White,⁶⁴ J. R. Wilson,⁶⁴ A. Randle-Conde,⁶⁵ S. J. Sekula,⁶⁵ M. Bellis,⁶⁶ J. F. Benitez,⁶⁶ P. R. Burchat,⁶⁶ T. S. Miyashita,⁶⁶ M. S. Alam,⁶⁷ J. A. Ernst,⁶⁷ R. Gorodeisky,⁶⁸ N. Guttman,⁶⁸ D. R. Peimer,⁶⁸ A. Soffer,⁶⁸ P. Lund,⁶⁹ S. M. Spanier,⁶⁹ R. Eckmann,⁷⁰ J. L. Ritchie,⁷⁰ A. M. Ruland,⁷⁰ C. J. Schilling,⁷⁰ R. F. Schwitters,⁷⁰ B. C. Wray,⁷⁰ J. M. Izen,⁷¹ X. C. Lou,⁷¹ F. Bianchi,^{72a,72b} D. Gamba,^{72a,72b} L. Lanceri,^{73a,73b} L. Vitale,^{73a,73b} F. Martinez-Vidal,⁷⁴ A. Oyanguren,⁷⁴ H. Ahmed,⁷⁵ J. Albert,⁷⁵ Sw. Banerjee,⁷⁵ H. H. F. Choi,⁷⁵

G. J. King,⁷⁵ R. Kowalewski,⁷⁵ M. J. Lewczuk,⁷⁵ I. M. Nugent,⁷⁵ J. M. Roney,⁷⁵ R. J. Sobie,⁷⁵ N. Tasneem,⁷⁵
 T. J. Gershon,⁷⁶ P. F. Harrison,⁷⁶ T. E. Latham,⁷⁶ E. M. T. Puccio,⁷⁶ H. R. Band,⁷⁷ S. Dasu,⁷⁷ Y. Pan,⁷⁷
 R. Prepost,⁷⁷ and S. L. Wu⁷⁷

(BABAR Collaboration)

- ¹Laboratoire d'Annecy-le-Vieux de Physique des Particules (LAPP), Université de Savoie, CNRS/IN2P3, F-74941 Annecy-Le-Vieux, France
- ²Universitat de Barcelona, Facultat de Física, Departament ECM, E-08028 Barcelona, Spain
- ^{3a}INFN Sezione di Bari, I-70126 Bari, Italy
- ^{3b}Dipartimento di Fisica, Università di Bari, I-70126 Bari, Italy
- ⁴University of Bergen, Institute of Physics, N-5007 Bergen, Norway
- ⁵Lawrence Berkeley National Laboratory and University of California, Berkeley, California 94720, USA
- ⁶Ruhr Universität Bochum, Institut für Experimentalphysik 1, D-44780 Bochum, Germany
- ⁷University of British Columbia, Vancouver, British Columbia, Canada V6T 1Z1
- ⁸Brunel University, Uxbridge, Middlesex UB8 3PH, United Kingdom
- ⁹Budker Institute of Nuclear Physics, Novosibirsk 630090, Russia
- ¹⁰University of California at Irvine, Irvine, California 92697, USA
- ¹¹University of California at Riverside, Riverside, California 92521, USA
- ¹²University of California at Santa Barbara, Santa Barbara, California 93106, USA
- ¹³University of California at Santa Cruz, Institute for Particle Physics, Santa Cruz, California 95064, USA
- ¹⁴California Institute of Technology, Pasadena, California 91125, USA
- ¹⁵University of Cincinnati, Cincinnati, Ohio 45221, USA
- ¹⁶University of Colorado, Boulder, Colorado 80309, USA
- ¹⁷Colorado State University, Fort Collins, Colorado 80523, USA
- ¹⁸Technische Universität Dortmund, Fakultät Physik, D-44221 Dortmund, Germany
- ¹⁹Technische Universität Dresden, Institut für Kern- und Teilchenphysik, D-01062 Dresden, Germany
- ²⁰Laboratoire Leprince-Ringuet, Ecole Polytechnique, CNRS/IN2P3, F-91128 Palaiseau, France
- ²¹University of Edinburgh, Edinburgh EH9 3JZ, United Kingdom
- ^{22a}INFN Sezione di Ferrara, I-44100 Ferrara, Italy
- ^{22b}Dipartimento di Fisica, Università di Ferrara, I-44100 Ferrara, Italy
- ²³INFN Laboratori Nazionali di Frascati, I-00044 Frascati, Italy
- ^{24a}INFN Sezione di Genova, I-16146 Genova, Italy
- ^{24b}Dipartimento di Fisica, Università di Genova, I-16146 Genova, Italy
- ²⁵Indian Institute of Technology Guwahati, Guwahati, Assam, 781 039, India
- ²⁶Harvard University, Cambridge, Massachusetts 02138, USA
- ²⁷Harvey Mudd College, Claremont, California 91711
- ²⁸Universität Heidelberg, Physikalisches Institut, Philosophenweg 12, D-69120 Heidelberg, Germany
- ²⁹Humboldt-Universität zu Berlin, Institut für Physik, Newtonstr. 15, D-12489 Berlin, Germany
- ³⁰Imperial College London, London, SW7 2AZ, United Kingdom
- ³¹University of Iowa, Iowa City, Iowa 52242, USA
- ³²Iowa State University, Ames, Iowa 50011-3160, USA
- ³³Johns Hopkins University, Baltimore, Maryland 21218, USA
- ³⁴Laboratoire de l'Accélérateur Linéaire, IN2P3/CNRS et Université Paris-Sud 11, Centre Scientifique d'Orsay, B. P. 34, F-91898 Orsay Cedex, France
- ³⁵Lawrence Livermore National Laboratory, Livermore, California 94550, USA
- ³⁶University of Liverpool, Liverpool L69 7ZE, United Kingdom
- ³⁷Queen Mary, University of London, London, E1 4NS, United Kingdom
- ³⁸University of London, Royal Holloway and Bedford New College, Egham, Surrey TW20 0EX, United Kingdom
- ³⁹University of Louisville, Louisville, Kentucky 40292, USA
- ⁴⁰Johannes Gutenberg-Universität Mainz, Institut für Kernphysik, D-55099 Mainz, Germany
- ⁴¹University of Manchester, Manchester M13 9PL, United Kingdom
- ⁴²University of Maryland, College Park, Maryland 20742, USA
- ⁴³University of Massachusetts, Amherst, Massachusetts 01003, USA
- ⁴⁴Massachusetts Institute of Technology, Laboratory for Nuclear Science, Cambridge, Massachusetts 02139, USA
- ⁴⁵McGill University, Montréal, Québec, Canada H3A 2T8
- ^{46a}INFN Sezione di Milano, I-20133 Milano, Italy
- ^{46b}Dipartimento di Fisica, Università di Milano, I-20133 Milano, Italy
- ⁴⁷University of Mississippi, University, Mississippi 38677, USA

- ⁴⁸*Université de Montréal, Physique des Particules, Montréal, Québec, Canada H3C 3J7*
^{49a}*INFN Sezione di Napoli, I-80126 Napoli, Italy*
^{49b}*Dipartimento di Scienze Fisiche, Università di Napoli Federico II, I-80126 Napoli, Italy*
⁵⁰*NIKHEF, National Institute for Nuclear Physics and High Energy Physics, NL-1009 DB Amsterdam, The Netherlands*
⁵¹*University of Notre Dame, Notre Dame, Indiana 46556, USA*
⁵²*Ohio State University, Columbus, Ohio 43210, USA*
⁵³*University of Oregon, Eugene, Oregon 97403, USA*
^{54a}*INFN Sezione di Padova, I-35131 Padova, Italy*
^{54b}*Dipartimento di Fisica, Università di Padova, I-35131 Padova, Italy*
⁵⁵*Laboratoire de Physique Nucléaire et de Hautes Energies, IN2P3/CNRS, Université Pierre et Marie Curie-Paris6, Université Denis Diderot-Paris7, F-75252 Paris, France*
^{56a}*INFN Sezione di Perugia, I-06100 Perugia, Italy*
^{56b}*Dipartimento di Fisica, Università di Perugia, I-06100 Perugia, Italy*
^{57a}*INFN Sezione di Pisa, I-56127 Pisa, Italy*
^{57b}*Dipartimento di Fisica, Università di Pisa, I-56127 Pisa, Italy*
^{57c}*Scuola Normale Superiore di Pisa, I-56127 Pisa, Italy*
⁵⁸*Princeton University, Princeton, New Jersey 08544, USA*
^{59a}*INFN Sezione di Roma, I-00185 Roma, Italy*
^{59b}*Dipartimento di Fisica, Università di Roma La Sapienza, I-00185 Roma, Italy*
⁶⁰*Universität Rostock, D-18051 Rostock, Germany*
⁶¹*Rutherford Appleton Laboratory, Chilton, Didcot, Oxon, OX11 0QX, United Kingdom*
⁶²*CEA, Irfu, SPP, Centre de Saclay, F-91191 Gif-sur-Yvette, France*
⁶³*SLAC National Accelerator Laboratory, Stanford, California 94309 USA*
⁶⁴*University of South Carolina, Columbia, South Carolina 29208, USA*
⁶⁵*Southern Methodist University, Dallas, Texas 75275, USA*
⁶⁶*Stanford University, Stanford, California 94305-4060, USA*
⁶⁷*State University of New York, Albany, New York 12222, USA*
⁶⁸*Tel Aviv University, School of Physics and Astronomy, Tel Aviv, 69978, Israel*
⁶⁹*University of Tennessee, Knoxville, Tennessee 37996, USA*
⁷⁰*University of Texas at Austin, Austin, Texas 78712, USA*
⁷¹*University of Texas at Dallas, Richardson, Texas 75083, USA*
^{72a}*INFN Sezione di Torino, I-10125 Torino, Italy*
^{72b}*Dipartimento di Fisica Sperimentale, Università di Torino, I-10125 Torino, Italy*
^{73a}*INFN Sezione di Trieste, I-34127 Trieste, Italy*
^{73b}*Dipartimento di Fisica, Università di Trieste, I-34127 Trieste, Italy*
⁷⁴*IFIC, Universitat de Valencia-CSIC, E-46071 Valencia, Spain*
⁷⁵*University of Victoria, Victoria, British Columbia, Canada V8W 3P6*
⁷⁶*Department of Physics, University of Warwick, Coventry CV4 7AL, United Kingdom*
⁷⁷*University of Wisconsin, Madison, Wisconsin 53706, USA*

(Received 26 October 2011; published 3 January 2012)

We report a measurement of the inclusive semileptonic branching fraction of the B_s meson using data collected with the BABAR detector in the center-of-mass energy region above the $\Upsilon(4S)$ resonance. We use the inclusive yield of ϕ mesons and the ϕ yield in association with a high-momentum lepton to perform a simultaneous measurement of the semileptonic branching fraction and the production rate of B_s mesons relative to all B mesons as a function of center-of-mass energy. The inclusive semileptonic branching fraction of the B_s meson is determined to be $\mathcal{B}(B_s \rightarrow \ell \nu X) = 9.5^{+2.5}_{-2.0}(\text{stat})^{+1.1}_{-1.9}(\text{syst})\%$, where ℓ indicates the average of e and μ .

DOI: 10.1103/PhysRevD.85.011101

PACS numbers: 14.40.Nd, 13.20.He

*Now at Temple University, Philadelphia, PA 19122, USA

†Also with Università di Perugia, Dipartimento di Fisica, Perugia, Italy

‡Now at the University of Huddersfield, Huddersfield HD1 3DH, UK

§Now at University of South Alabama, Mobile, AL 36688, USA

||Also with Università di Sassari, Sassari, Italy

Semileptonic decays of heavy-flavored hadrons serve as a powerful probe of the electroweak and strong interactions and are essential to determinations of Cabibbo-Kobayashi-Maskawa matrix elements (see, for example, “Determination of V_{cb} and V_{ub} ” in Ref. [1]). The inclusive semileptonic branching fractions of the B_d and B_u mesons are measured to high precision by experiments operating at the $\Upsilon(4S)$ resonance, which decays almost exclusively to $B\bar{B}$ pairs (here and throughout this note, $B\bar{B}$ refers to $B_d\bar{B}_d$ and

$B_u\bar{B}_u$). However, lacking an analogous production mechanism, information on branching fractions of the B_s meson remains scarce nearly two decades after its first observation [1]. Here we report a measurement of the inclusive semileptonic branching fraction of the B_s meson using data collected with the *BABAR* detector at the PEP-II asymmetric-energy electron-positron collider, located at the SLAC National Accelerator Laboratory. The data were collected in a scan of center-of-mass (CM) energies above the $Y(4S)$ resonance, including the region near the $B_s\bar{B}_s$ threshold. As ϕ mesons are particularly abundant in B_s decays due to the Cabibbo-Kobayashi-Maskawa-favored $B_s \rightarrow D_s$ transition, the inclusive production rate of ϕ mesons and the rate of ϕ mesons produced in association with a high-momentum electron or muon can be used to simultaneously determine the B_s semileptonic branching fraction and the B_s production fraction as a function of the CM energy E_{CM} .

The energy scan data correspond to an integrated luminosity of 4.25 fb^{-1} collected in 2008 in 5 MeV steps in the range $10.54 \text{ GeV} \leq E_{\text{CM}} \leq 11.2 \text{ GeV}$. In a previous study [2], we presented a measurement of the inclusive b quark production cross section $R_b = \sigma(e^+e^- \rightarrow b\bar{b})/\sigma^0(e^+e^- \rightarrow \mu^+\mu^-)$ in this energy range, using this same data sample (σ^0 is the zeroth-order QED cross section). In the present study, we also make use of 18.55 fb^{-1} of data collected in 2007 at the peak of the $Y(4S)$ resonance, and 7.89 fb^{-1} collected 40 MeV below the $Y(4S)$, to evaluate backgrounds from continuum ($e^+e^- \rightarrow q\bar{q}$, $q = u, d, s, c$ quark production) and $B\bar{B}$ events. We choose below-resonance data for which detector conditions most closely resemble those of the scan, and on-resonance data corresponding to roughly twice the luminosity of the below-resonance sample. The sizes of these samples are sufficient to reduce the corresponding systematic uncertainties below those associated with irreducible sources.

The *BABAR* detector is described in detail elsewhere [3]. The tracking system is composed of a five-layer silicon vertex tracker (SVT) and a 40-layer drift chamber (DCH) in a 1.5-Tesla axial magnetic field. The SVT provides a precise determination of the track parameters near the interaction point and standalone tracking for charged particle transverse momenta (p_t) down to 50 MeV/ c . The DCH provides a 98% efficient measurement of charged particles with $p_t > 500 \text{ MeV}/c$. The p_t resolution is $\sigma_{p_t}/p_t = (0.13 \cdot p_t + 0.45)\%$. Hadron and muon identification in *BABAR* is achieved by using a likelihood-based algorithm exploiting specific ionization measured in the SVT and the DCH in combination with information from an instrumented magnetic-flux return and the Cherenkov angle obtained from the detector of internally reflected Cherenkov light. Electron identification is provided by a combination of tracking and information from the CsI(Tl) electromagnetic calorimeter, which also serves to measure photon energies. For the evaluation of event reconstruction

efficiencies across the scan range, simulated samples of $e^+e^- \rightarrow \mu^+\mu^-$, continuum, and $e^+e^- \rightarrow B_q^{(*)}\bar{B}_q^{(*)}$, $q = u, d, s$ events, created with the KK2F [4], JETSET [5], and EVTGEN [6] event generators, respectively, are processed through a GEANT4 [7] simulation of the *BABAR* detector.

For this measurement, we present the scan data as a function of E_{CM} in bins of 15 MeV. In each bin we measure the number of $B\bar{B}$ -like events (defined below), the number of such events containing a ϕ meson, and the number of events in which the ϕ meson is accompanied by a charged lepton candidate. The results are normalized to the number of $e^+e^- \rightarrow \mu^+\mu^-$ events in the same energy bin so that the luminosity dependence in each bin is removed. These three measurements are used to extract the fractional number of $B_s\bar{B}_s$ events and the semileptonic branching fraction $\mathcal{B}(B_s \rightarrow \ell\nu X)$. The procedure is described in detail below.

To suppress QED background, events are preselected with a multihadronic event filter optimized to select $B\bar{B}$ and $B_s\bar{B}_s$ events. The filter requires a minimum number of charged tracks in the event (3), a minimum total event energy (4.5 GeV), a well-identified primary vertex near the expected collision point, and a maximum value of the ratio of the second to zeroth Fox-Wolfram moments [8] ($R_2 < 0.2$) calculated in the CM frame using both charged tracks and energy depositions in the calorimeter, where the latter are required not to be associated with a track.

A different preselection is used to identify muon pair events. Events passing this selection must have at least two tracks. The two highest momentum tracks are required to be back-to-back in the CM frame to within 10 degrees, appear at large angles to the beam axis ($|\cos\theta_{\text{CM}}| < 0.7486$), and have an invariant mass greater than $7.5 \text{ GeV}/c^2$. In addition, we require that less than 1 GeV be deposited in the electromagnetic calorimeter. This selection is 43% efficient for simulated $\mu^+\mu^-$ events while rejecting virtually all continuum events.

Candidate ϕ mesons are reconstructed in the $\phi \rightarrow K^+K^-$ decay mode, by forming pairs of oppositely charged tracks that are consistent with the kaon hypothesis. In each event, the ϕ candidate with the best-identified K^\pm daughters is selected by assigning a weight to each K^\pm based on the particle identification criteria. The ϕ candidate with the largest sum of kaon weights is selected. The invariant mass distribution of these candidates is used to determine the ϕ yield in a given E_{CM} bin using a maximum likelihood fit. Events containing ϕ candidates and an electron or muon candidate with a CM momentum exceeding 900 MeV/ c are used to determine the yield of events with both a ϕ and a lepton (ϕ -lepton events). The requirement on the lepton momentum suppresses background from semileptonic charm decays.

Figure 1 shows, as an example, the K^+K^- invariant mass distribution for (a) all ϕ candidates, and (b) ϕ -lepton candidates, in the energy bin $10.8275 < E_{\text{CM}} < 10.8425 \text{ GeV}$. These mass distributions are fit to the function

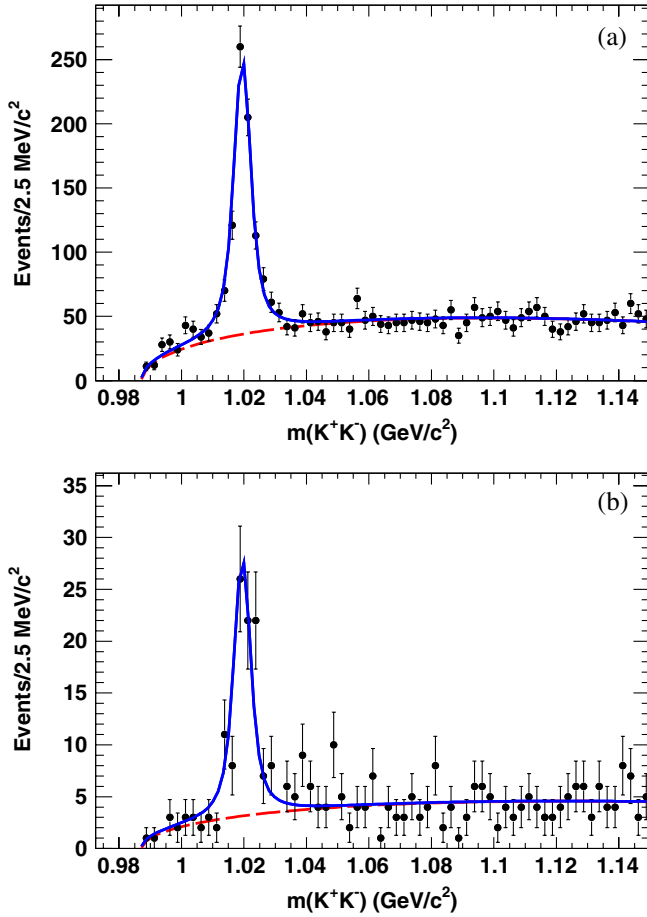


FIG. 1 (color online). Invariant mass distribution of $\phi \rightarrow K^+K^-$ candidates in the energy bin $10.8275 \text{ GeV} \leq E_{\text{CM}} \leq 10.8425 \text{ GeV}$: (a) inclusive ϕ candidates; (b) ϕ -lepton candidates. The background shape is shown by the dashed curve and the total fit by the solid curve.

$$f(M; N, b, c) \equiv NV(m_{KK}; m_\phi, \Gamma_\phi, \sigma) + Nc(1 + bm_{KK})\sqrt{1 - \left(\frac{2m_K}{m_{KK}}\right)^2}, \quad (1)$$

with m_K the world-average mass value [1] of the K^\pm . $V(m_{KK}; m_\phi, \Gamma_\phi, \sigma)$ is a Voigt profile (the convolution of a Breit-Wigner function $1/((m_{KK} - m_\phi)^2 + \Gamma_\phi^2/4)$ with a Gaussian resolution function) normalized to unity, so that N is the number of events in the peak. We fix the mean (m_ϕ) and Breit-Wigner width (Γ_ϕ) to the world-average values of the ϕ mass and natural width [1], and the width of the Gaussian resolution (σ) by first performing all of the ϕ fits with the parameter left free, then fixing it to the weighted mean of all of the values obtained across the scan. The value in data determined by this method is $\sigma = 1.61 \pm 0.04(\text{stat}) \text{ MeV}/c^2$. The combinatoric background is modeled as the product of a linear term and a threshold cutoff function parameterized by the slope of the linear term (b) and a relative scaling (c).

To determine the ϕ and ϕ -lepton yields from B decays in each E_{CM} bin, the contribution of continuum events is subtracted. This is achieved by using the data collected below the $Y(4S)$ described above. The event, ϕ , and ϕ -lepton yields are measured in this data set following the same procedures described above. These yields are corrected for the energy dependence of the reconstruction efficiencies and are then subtracted from the scan yields in each E_{CM} bin. This procedure neglects the different energy dependence of a small component of the hadronic and dimuon cross sections, primarily due to the presence of initial state radiative (ISR) $e^+e^- \rightarrow \gamma Y(1S, 2S, 3S)$ and two photon $e^+e^- \rightarrow e^+e^-\gamma^*\gamma^* \rightarrow e^+e^-X_h$ events, which do not scale according to $1/E_{\text{CM}}^2$. The effect of these contributions is to introduce a small energy dependence on the amount to be subtracted from each bin. The average size of this effect is estimated to be less than 2% of the below-resonance event yield. The impact on the result is taken as a systematic uncertainty.

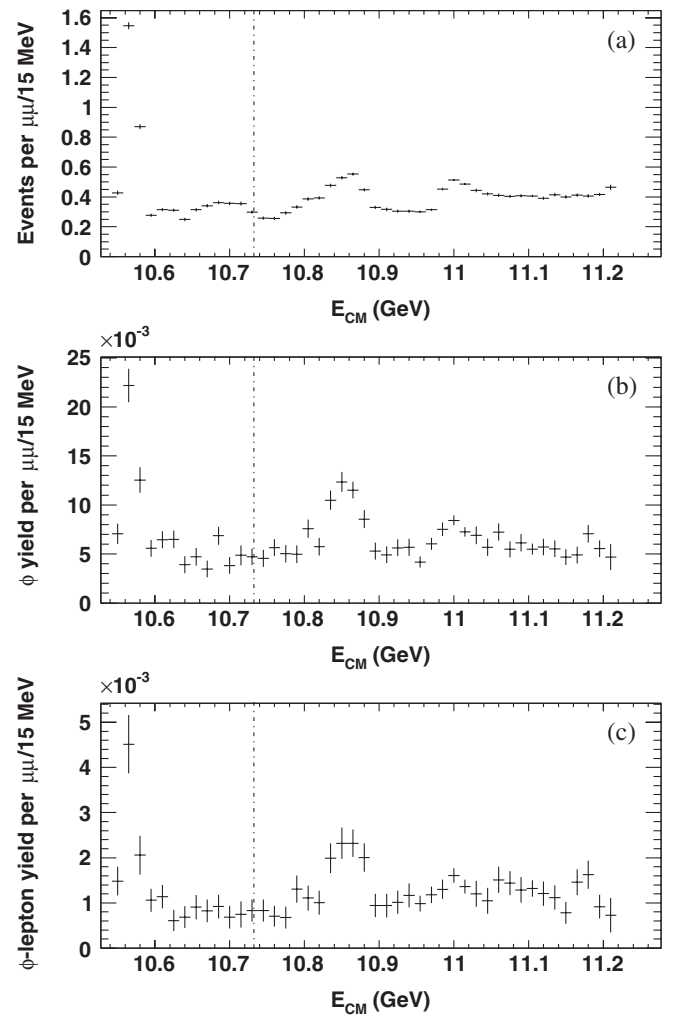


FIG. 2. Relative (a) event, (b) ϕ , and (c) ϕ -lepton yields, normalized to the $\mu^+\mu^-$ yields. Corrections for detector efficiency have not been applied. The dotted vertical line indicates the B_s production threshold.

The normalized event, ϕ , and ϕ -lepton yields after the continuum subtraction are presented in Fig. 2. These three quantities, denoted C_h , C_ϕ and $C_{\phi\ell}$ respectively, can be expressed in terms of contributions from events containing $B_{u,d}^{(*)}$ and $B_s^{(*)}$ events, the cross section ratio $R_B \equiv \sum_{q=\{u,d,s\}} \sigma(e^+e^- \rightarrow B_q \bar{B}_q) / \sigma_{\mu^+\mu^-}$, and the related reconstruction efficiencies, as follows:

$$C_h = R_B [f_s \epsilon_h^s + (1 - f_s) \epsilon_h] \quad (2)$$

$$C_\phi = R_B [f_s \epsilon_\phi^s P(B_s \bar{B}_s \rightarrow \phi X) + (1 - f_s) \epsilon_\phi P(B \bar{B} \rightarrow \phi X)] \quad (3)$$

$$C_{\phi\ell} = R_B [f_s \epsilon_{\phi\ell}^s P(B_s \bar{B}_s \rightarrow \phi \ell X) + (1 - f_s) \epsilon_{\phi\ell} P(B \bar{B} \rightarrow \phi \ell X)] \quad (4)$$

(with energy dependence implicit in all terms here and elsewhere), where

$$f_s \equiv \frac{N_{B_s}}{N_{B_u} + N_{B_d} + N_{B_s}} \quad (5)$$

and ϵ_X (ϵ_X^s) is the efficiency for a $B_{u,d}$ (B_s) pair to contribute to the event, ϕ or ϕ -lepton yield. The efficiencies are estimated from simulation, while $P(B \bar{B} \rightarrow \phi X)$ and $P(B \bar{B} \rightarrow \phi \ell X)$, which are the probabilities that a ϕ or a ϕ -lepton combination is produced in an event with a $B \bar{B}$ pair, are measured using the $Y(4S)$ data sample described above. Specifically, we determine the ϕ and ϕ -lepton yields in the $Y(4S)$ data. We then apply Eqs. (2)–(4) with $f_s = 0$ to extract $\epsilon_\phi P(B \bar{B} \rightarrow \phi X)$ and $\epsilon_{\phi\ell} P(B \bar{B} \rightarrow \phi \ell X)$. Simulations are used to extrapolate the values of the efficiencies to other energies.

The remaining unknown quantities of interest are the probabilities $P(B_s \bar{B}_s \rightarrow \phi X)$ and $P(B_s \bar{B}_s \rightarrow \phi \ell X)$ that a $B_s \bar{B}_s$ pair will yield a ϕ or ϕ -lepton event. To estimate $P(B_s \bar{B}_s \rightarrow \phi X)$ we use the current world averages [1] of the inclusive branching fractions $\mathcal{B}(B_s \rightarrow D_s X)$, $\mathcal{B}(D_s \rightarrow \phi X)$, and $\mathcal{B}(D \rightarrow \phi X)$. Here and in the following D refers to the sum of D^\pm and D^0 contributions. Also needed are estimates of the unmeasured branching fractions $\mathcal{B}(B_s \rightarrow c \bar{c} \phi)$ and $\mathcal{B}(B_s \rightarrow DD_s X)$. The former quantity accounts for direct $B_s \rightarrow \phi$ production, a substantial fraction of which arises from B_s to charmonium decays. We use the central value from the simulation, 1.7%, which is roughly consistent with charmonium production in the B system. For the latter quantity we use a naive quark model prediction of 15% for $b \rightarrow cc s$.

The inclusive ϕ yield in B_s decays can be expressed as

$$\begin{aligned} P(B_s \rightarrow \phi X) &= \mathcal{B}(B_s \rightarrow D_s^{(*)} X) \mathcal{B}(D_s \rightarrow \phi X) \\ &+ \mathcal{B}(B_s \rightarrow c \bar{c} \phi) \\ &+ \mathcal{B}(B_s \rightarrow DD_s X) \mathcal{B}(D \rightarrow \phi X), \quad (6) \end{aligned}$$

from which we determine

$$P(B_s \bar{B}_s \rightarrow \phi X) = 2P(B_s \rightarrow \phi X) - P(B_s \rightarrow \phi X)^2. \quad (7)$$

The unknown quantities in Eqs. (2) and (3) are f_s and the common normalization R_B . The ratio f_s can be determined as a function of E_{CM} by eliminating R_B between the two equations. The result is presented in Fig. 3. The ratio f_s peaks around the $Y(5S)$ mass. The total excess below the $B_s \bar{B}_s$ threshold and deficit above 11 GeV are consistent with zero within 1.5 and 1.3 standard deviations, respectively.

Using Eq. (4), a χ^2 is constructed from the measured and expected values of $P(B_s \bar{B}_s \rightarrow \phi \ell X)$ across the entire scan. The χ^2 is minimized with respect to $\mathcal{B}(B_s \rightarrow \ell \nu X)$. The following processes contribute to $C_{\phi\ell}$ from $B_s \bar{B}_s$ events: primary leptons originating from a B_s semileptonic decay, secondary leptons resulting from semileptonic decays of charmed mesons, and π^\pm or K^\pm misidentified as e^\pm or μ^\pm . The contribution from primary leptons arises from events where one or both B_s mesons decay semileptonically, and we determine the ϕ -lepton efficiency for each case (denoted $\epsilon_{\phi\ell}^s$ for one semileptonic decay and $\epsilon_{\phi\ell\ell}^s$ for two). It is found that $\epsilon_{\phi\ell}^s$ ranges from 8.5%–10% and $\epsilon_{\phi\ell\ell}^s$ is about 10%.

For the secondary lepton contribution, we consider events with up to two leptons coming from D^\pm , D^0 or D_s^\pm decays. The selection efficiency in this case is estimated as the product of the ϕ reconstruction efficiency in $B_s \bar{B}_s$ events in which neither B_s decays semileptonically but a lepton candidate is identified (referred to below as ϵ_ϕ^D), and a lepton detection efficiency determined from simulation (ϵ_ℓ^D). It is found that ϵ_ϕ^D lies in the range 15%–16.5%, and ϵ_ℓ^D in the range 8%–9.5% per lepton. The contribution from hadrons that are misidentified as leptons is estimated from simulation to be 3.3% of the ϕ -lepton candidates in $B_s \bar{B}_s$ events.

For the expected and measured ϕ yields, we find

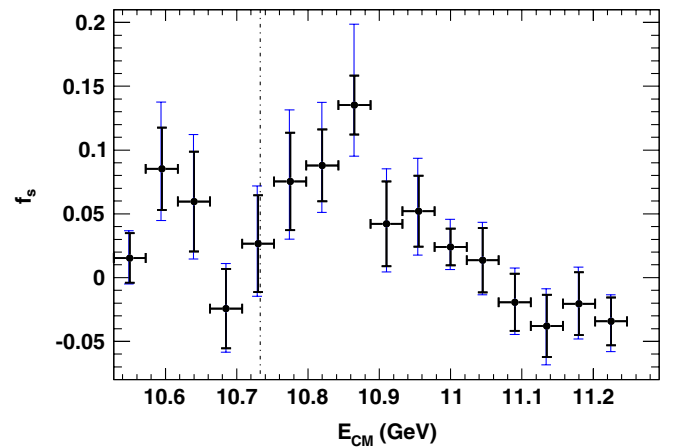


FIG. 3 (color online). Results for the fraction f_s as a function of E_{CM} . The inner error bars show the statistical uncertainties and the outer error bars the statistical and systematic uncertainties added in quadrature. The dotted line denotes the B_s threshold.

$$\begin{aligned} \epsilon_{\phi\ell}^s P(B_s \bar{B}_s \rightarrow \phi \ell X)_{\text{Primary}} &= (2\epsilon_{\phi\ell}^s - \epsilon_{\phi\ell\ell}^s) \mathcal{B}(D_s \rightarrow \phi X) [-2 + \mathcal{B}(D_s \rightarrow \phi X)] [\mathcal{B}(B_s \rightarrow \ell\nu X)]^2 \\ &+ \mathcal{B}(B_s \rightarrow \ell\nu X) \epsilon_{\phi\ell}^s [\mathcal{B}(D_s \rightarrow \phi X) + [1 - \mathcal{B}(D_s \rightarrow \phi X)] P(B_s \rightarrow \phi X)], \end{aligned} \quad (8)$$

$$\begin{aligned} \epsilon_{\phi\ell}^s P(B_s \bar{B}_s \rightarrow \phi \ell X)_{\text{Secondary}} &= 2\epsilon_{\ell}^D \epsilon_{\phi}^D \{ [\mathcal{B}(D_s \rightarrow \ell\nu\phi) + \mathcal{B}(D_s \rightarrow \ell\nu X) \mathcal{B}(D_s \rightarrow \phi X) \\ &- \mathcal{B}(D_s \rightarrow \ell\nu\phi) \mathcal{B}(D_s \rightarrow \phi X)] [\mathcal{B}(B_s \rightarrow \ell\nu X)]^2 + [P(B_s \rightarrow \phi X) (\mathcal{B}(D_s \rightarrow \ell\nu\phi) \\ &- \mathcal{B}(D_s \rightarrow \ell\nu X)) - \mathcal{B}(D_s \rightarrow \ell\nu\phi) - \mathcal{B}(B_s \rightarrow D_s X) \mathcal{B}(D_s \rightarrow \ell\nu\phi) \\ &- \mathcal{B}(B_s \rightarrow D_s X) \mathcal{B}(D_s \rightarrow \ell\nu X) \mathcal{B}(D_s \rightarrow \phi X) + \mathcal{B}(B_s \rightarrow D_s X) \mathcal{B}(D_s \rightarrow \ell\nu\phi) \\ &\times \mathcal{B}(D_s \rightarrow \phi X) + (\mathcal{B}(D_s \rightarrow \phi X) - 2) \\ &\times \sum_{i \in u, d, s} \mathcal{B}(B_s \rightarrow D_s^{(*)-} D_i(X)) \mathcal{B}(D_i \rightarrow \ell\nu X)] \mathcal{B}(B_s \rightarrow \ell\nu X) \\ &+ \mathcal{B}(B_s \rightarrow D_s X) P(B_s \rightarrow \phi X) [\mathcal{B}(D_s \rightarrow \ell\nu X) - \mathcal{B}(D_s \rightarrow \ell\nu\phi)] \\ &+ \mathcal{B}(B_s \rightarrow D_s X) \mathcal{B}(D_s \rightarrow \ell\nu\phi) + [\mathcal{B}(B_s \rightarrow \phi X) + \mathcal{B}(D_s \rightarrow \phi X) \\ &- P(B_s \rightarrow \phi X) \mathcal{B}(D_s \rightarrow \phi X)] \sum_{i \in u, d, s} \mathcal{B}(B_s \rightarrow D_s^{(*)-} D_i(X)) \mathcal{B}(D_i \rightarrow \ell\nu X) \}, \end{aligned} \quad (9)$$

$$\begin{aligned} \epsilon_{\phi\ell}^s P(B_s \bar{B}_s \rightarrow \phi \ell X)_{\text{Expected}} &= \{ \epsilon_{\phi\ell}^s \times 0.591 \times \mathcal{B}(B_s \rightarrow \ell\nu X) - (2\epsilon_{\phi\ell}^s - \epsilon_{\phi\ell\ell}^s) \times 0.289 \times (\mathcal{B}(B_s \rightarrow \ell\nu X))^2 \\ &+ \epsilon_{\phi}^D \epsilon_{\ell}^D [0.1375 - 0.2721 \times \mathcal{B}(B_s \rightarrow \ell\nu X) + 0.1339 \times (\mathcal{B}(B_s \rightarrow \ell\nu X))^2] \}, \end{aligned} \quad (10)$$

$$\epsilon_{\phi\ell}^s P(B_s \bar{B}_s \rightarrow \phi \ell X)_{\text{Measured}} = (1 - 0.033) \left(C_{\phi\ell} \frac{f_s \epsilon_h^s + (1 - f_s) \epsilon_h}{f_s C_h} - \frac{(1 - f_s) \epsilon_{\phi\ell} P(B\bar{B} \rightarrow \phi \ell X)}{f_s} \right), \quad (11)$$

where Eq. (10) is the sum of Eqs. (8) and (9) after substituting the values of known quantities. The first line in Eq. (10) expresses the contribution from primary leptons and the second that from secondary leptons. Equations (10) and (11) describe the measured and expected values used to form the χ^2 to be minimized, along with the statistical uncertainties of each of the measured quantities and the uncertainties in the energy-dependent efficiencies.

The expression in Eq. (10) for the expected value of $\epsilon_{\phi\ell}^s P(B_s \bar{B}_s \rightarrow \phi \ell X)$ is quadratic in the unknown $\mathcal{B}(B_s \rightarrow \ell\nu X)$, and so a χ^2 formed from the deviation of the expected from the measured values, summed over all bins above the $B_s \bar{B}_s$ threshold, is quartic in this unknown. Minimizing the χ^2 with respect to the B_s semileptonic branching fraction we find $\mathcal{B}(B_s \rightarrow \ell\nu X) = 9.5_{-2.0}^{+2.5}\%$. Figure 4 shows the dependence of χ^2 on $\mathcal{B}(B_s \rightarrow \ell\nu X)$.

Systematic uncertainties are summarized in Table I and include the contributions described below.

- (i) Uncertainties for branching fractions, which are either taken from Ref. [1] when known, or assumed to be 50% for $\mathcal{B}(B_s \rightarrow c\bar{c}\phi)$ and $\mathcal{B}(B_s \rightarrow DD_s X)$. These are separately listed in Table I, as is $\mathcal{B}(B_s \rightarrow D_s X)$, which contributes a very large uncertainty compared to the other branching fractions.
- (ii) Requirements used in the event preselection, including the lepton momentum requirement. The uncertainty due to the lepton momentum requirement dominates in this group, and reflects the dependence

of the result on the decay model used to simulate B_s semileptonic decays.

- (iii) Fixed parameters used in the fits to m_{KK} , including m_{ϕ} , Γ_{ϕ} , σ .
- (iv) The parameterization of the background and absence of a term in the fit corresponding to threshold contributions from light scalars.

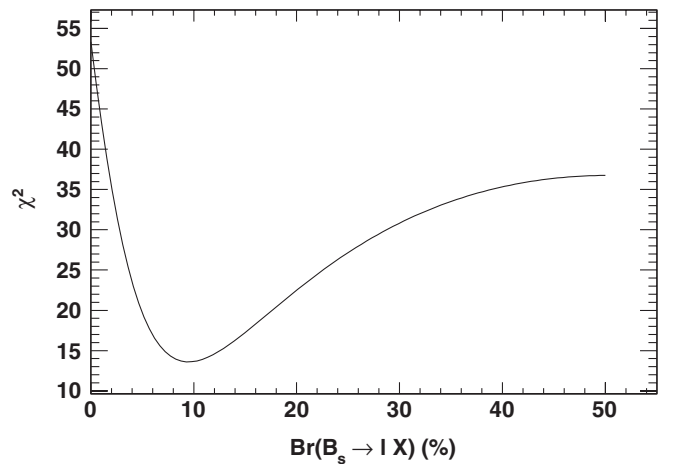


FIG. 4. χ^2 formed from the measured and expected yields, as described in the text, as a function of the semileptonic branching fraction. Note that since we express the branching fraction as the average of the e and μ channels, the physical bound is 50%.

TABLE I. Relative multiplicative and additive systematic uncertainties for the measurement of $\mathcal{B}(B_s \rightarrow \ell \nu X)$.

Multiplicative systematics	Relative uncertainty (%)
$\mathcal{B}(B_s \rightarrow D_s^{(*)} X)$	+8.72/ - 13.58
$\mathcal{B}(B_s \rightarrow c \bar{c} \phi)$ (unmeasured)	± 3.20
$\mathcal{B}(B_s \rightarrow DD_s X)$ (unmeasured)	+1.12/ - 1.16
Other branching fractions	+0.52/ - 0.54
Event and lepton selection	+1.99/ - 2.85
Fixed fit parameters	+0.49/ - 0.15
Background parameterization	± 0.93
PID and lepton fake rate	± 3.21
$P(B_{u,d} \bar{B}_{u,d} \rightarrow \phi)$	+1.47/ - 1.69
Simulation branching fractions	± 2.59
ISR and 2γ background	+1.57/ - 7.14
Correction to event subtraction	+1.88/ - 4.59
Technique bias	+0.39/ - 10.00
<i>Total multiplicative</i>	(+10.87/ - 19.92)%
Additive systematics	Uncertainty ($\times 10^{-3}$)
Other branching fractions	+0.56/ - 0.64
$P(B_{u,d} \bar{B}_{u,d} \rightarrow \phi \ell \nu)$	+4.30/ - 3.90
<i>Total additive</i>	(+4.34/ - 3.95) $\times 10^{-3}$
<i>Total systematic</i>	(+11.20/ - 19.34) $\times 10^{-3}$

- (v) Uncertainties in particle identification (PID) efficiencies and hadron misidentification probabilities.
- (vi) The determination of $P(B\bar{B} \rightarrow \phi X)$ and $P(B\bar{B} \rightarrow \phi \ell X)$ in $Y(4S)$ data (these quantities are determined to 1% and 1.8% relative uncertainty).
- (vii) Sensitivity of efficiencies to differences in branching fractions implemented in simulation compared to their measured values.
- (viii) Uncertainties in the continuum-subtracted number of events due to ISR and two photon events, which do not follow a $1/E_{\text{CM}}^2$ energy dependence.
- (ix) A correction made to the continuum subtraction of the number of $B\bar{B}$ -like events due to an over-subtraction found in simulation studies. The size of this correction is about 1% of the amount to be subtracted; we use $\pm 100\%$ of this correction as a systematic uncertainty.

- (x) Possible bias in the χ^2 minimization technique at low statistics. First, evaluating the behavior of this method for extracting $\mathcal{B}(B_s \rightarrow \ell \nu X)$ for many pseudo-data samples derived from the simulated data set gives evidence for a small bias at low statistics. Second, it was found that the analysis performed in high statistics simulation tends to over-estimate $\mathcal{B}(B_s \rightarrow \ell \nu X)$ by an amount corresponding to half the statistical error reported.

To determine whether the uncertainties from these sources scale with the result or not, each was evaluated in a simulation sample with a higher semileptonic branching fraction and compared with the result in the normal simulation sample. It was found that the uncertainty from the determination of $P(B\bar{B} \rightarrow \phi \ell X)$ in $Y(4S)$ data does not scale with the branching fraction, nor does the uncertainty contributed by several of the input branching fractions. These are thus separated in Table I. The remaining uncertainties are found to scale with $\mathcal{B}(B_s \rightarrow \ell \nu X)$ and thus to be multiplicative.

Our final result for the inclusive semileptonic branching fraction is $9.5^{+2.5+1.1}_{-2.0-1.9}\%$, which is the average of the branching fractions to e and μ .

In conclusion, we performed a simultaneous measurement of the B_s semileptonic branching fraction and its production rates in the CM energy region from 10.56 GeV to 11.20 GeV. The semileptonic branching fraction is consistent with theoretical calculations in Refs. [9,10]. Our measurement of the B_s production rates are consistent with the predictions of coupled channel models [11], in which B_s production peaks near the $Y(5S)$ and is vanishingly small elsewhere.

We are grateful for the excellent luminosity and machine conditions provided by our PEP-II colleagues, and for the substantial dedicated effort from the computing organizations that support *BABAR*. The collaborating institutions wish to thank SLAC for its support and kind hospitality. This work is supported by DOE and NSF (USA), NSERC (Canada), CEA and CNRS-IN2P3 (France), BMBF and DFG (Germany), INFN (Italy), FOM (The Netherlands), NFR (Norway), MES (Russia), MICIIN (Spain), STFC (United Kingdom). Individuals have received support from the Marie Curie EIF (European Union), the A. P. Sloan Foundation (USA) and the Binational Science Foundation (USA-Israel).

[1] K. Nakamura *et al.* (Particle Data Group), *J. Phys. G* **37**, 075021 (2010).
[2] B. Aubert *et al.* (*BABAR* Collaboration), *Phys. Rev. Lett.* **102**, 012001 (2009).
[3] B. Aubert *et al.* (*BABAR* Collaboration), *Nucl. Instrum. Methods Phys. Res., Sect. A* **479**, 1 (2002).

[4] S. Jadach, B.F.L. Ward, and Z. Was, *Comput. Phys. Commun.* **130**, 260 (2000).
[5] T. Sjostrand, *Comput. Phys. Commun.* **82**, 74 (1994).
[6] D.J. Lange, *Nucl. Instrum. Methods Phys. Res., Sect. A* **462**, 152 (2001).

- [7] S. Agostinelli *et al.* (GEANT4 Collaboration), *Nucl. Instrum. Methods Phys. Res., Sect. A* **506**, 250 (2003).
- [8] G.C. Fox and S. Wolfram, *Phys. Rev. Lett.* **41**, 1581 (1978).
- [9] M. Gronau and J.L. Rosner, *Phys. Rev. D* **83**, 034025 (2011).
- [10] I.I. Bigi, Th. Mannel, and N. Uraltsev, *J. High Energy Phys.* **09** (2011) 012.
- [11] N.A. Törnqvist, *Phys. Rev. Lett.* **53**, 878 (1984).